Flavopiridol and Trastuzumab Synergistically Inhibit Proliferation of Breast Cancer Cells: Association with Selective Cooperative Inhibition of Cyclin D1-dependent Kinase and Akt Signaling Pathways[1]

Kongming Wu, Chenguang Wang, Mark D'Amico, Richard J. Lee, Chris Albanese, Richard G. Pestell, and Sridhar Mani[2]

Division of Hormone-dependent Tumor Biology [K. W., C. W., M. D., R. J. L., C. A., R. G. P., S. M.] and Albert Einstein Comprehensive Cancer Center [R. G. P., S. M.], Albert Einstein College of Medicine, Bronx, New York 10461

Abstract

Cyclin D1 is essential for Neu-induced cell growth and is induced by growth factors through Ras-dependent and Ras-independent signaling pathways (1). Because flavopiridol, a novel flavanoid cyclin-cyclin-dependent kinase inhibitor, may function through Ras-dependent and/or -independent pathways, we hypothesized that treatment of breast cancer cells with inhibitors of Neu signaling and flavopiridol might synergize to inhibit proliferation. Human breast cancer cell lines, which express high levels of endogenous Neu receptor, were treated with the anti-Neu antibody, trastuzumab, together with flavopiridol and subject to MTT assay. Cell lines were assayed for alterations in cell cycle by fluorescence-activated cell sorter and signaling proteins by Western blot. Flavopiridol and trastuzumab synergistically inhibited DNA synthesis, cellular proliferation, and contact-dependent growth. Cytotoxic synergy was observed independent of the sequence of addition of the two drugs to cultured cells. In SKBR3 cells, a combination of trastuzumab and flavopiridol inhibited the Ras-MAPK-Akt pathway, decreased cyclin D1 abundance, and kinase activity to a greater extent than either drug alone. Compared with single-agent treatment, combination treatment selectively inhibited Akt and pRB phosphorylation. Cytotoxic synergy was observed with flavopiridol plus LY294002 (selective phosphatidylinositol 3-kinase inhibitor) but not with PD98059 (selective mitogen-activated protein kinase kinase 1 inhibitor) suggesting that Akt inhibition may be important in synergy. Zinc-induced overexpression of cyclin D1 in T-47D ΔMTcycD1 cells were more resistant to drug-induced cell death when compared with vector-transfected T-47D ΔMT cells. Cyclin D1 overexpression reverses drug treatment induced cell cycle arrest in SKBR3 cells. Flavopiridol and trastuzumab yield cytotoxic synergy in human breast cancer cells overexpressing Neu. Cyclin D1 overexpression results in combination drug resistance. In addition, inhibition of Akt may prove to be a useful therapeutic strategy in combination with flavopiridol.

Introduction

Overexpression of the Neu receptor tyrosine kinase, resulting primarily from amplification of the HER-2/*neu* gene, is present in up to 30% of human breast tumors and is associated with poor prognosis (2). Neu receptor overexpression has been linked to chemoresistance and resistance to antiestrogens such as tamoxifen (3–6). Recently, trastuzumab, a humanized monoclonal antibody directed against the extracellular domain of the Neu receptor, was approved by the United States Food and Drug Administration for the treatment of metastatic breast cancer based on superior survival benefits as compared with conventional therapy (7). Hormone binding to receptor tyrosine kinase can activate at least five different independent signaling pathways (PLC-δ/phosphatidylinositol turnover; PI3K[3]; STAT91/ISGF-3; ras/raf/MAPK; and *src* family), and for most of these pathways there is evidence for nuclear gene activation (8–10). Cyclin D1 is a regulatory subunit of a holoenzyme that phosphorylates and inactivates the tumor suppressor, pRB, regulating a rate-limiting component in proliferation of cells (11). The two catalytic subunits (or Cdks), Cdk4 and Cdk6, encode heterodimeric partners of cyclin D1. Cyclin D1 is induced by a variety of proliferative and transforming signals such as Neu (1), Ras (12), Rac (13), Src (14), STATs (15, 16), β-catenin (17), wnt (18), and activating mutants of MAPK (19). These signals induce cyclin D1 transcription and protein accumulation. Cyclin D1 is degraded rapidly upon withdrawal of growth factors via the proteosome pathway (20). It has been pro-

Received 2/7/02; revised 5/7/02; accepted 5/28/02.
[1] This work was supported in part by NIH Grants RO1CA70896, RO1CA75503, RO1CA86072, and RO1CA86071 and awards from the Pfeiffer Foundation, Breast Cancer Alliance, and The Susan Komen Breast Cancer Foundation (to R. G. P.).
[2] To whom requests for reprints should be addressed, at Albert Einstein College of Medicine, Chanin 302, 1300 Morris Park Avenue, Bronx, NY 10461. Phone: (718) 430-8663; Fax: (718) 430-8674; E-mail: smani64@aol.com.

[3] The abbreviations used are: PI3K, phosphatidylinositol 3-kinase; Cdk, cyclin-dependent kinase; pRB, retinoblastoma protein; MAPK, mitogen-activated protein kinase; FBS, fetal bovine serum; CombI, combination index; GDI, guanine nucleotide dissociation inhibitor; FACS, fluorescence-activated cell sorter; ERK, extracellular signal-regulated kinase; MEK, MAPK kinase; JNK, c-Jun NH_2-terminal kinase; MTS, 3-(4,5-dimethylthiazol-2-yl)-5-(3-carboxymethoxyphenyl)-2-(4-sulfophenyl)-2*H*-tetrazolium, inner salt.

posed that sustained growth factor and oncogene induction of cyclin D1 may contribute to the transformed phenotype (11, 21, 22).

In a previous publication, we had shown that cyclin D1 antisense inhibited Neu-induced transformation in Rat 1 cells. Furthermore, growth of Neu-induced mammary carcinoma cells in nude mice was inhibited by cyclin D1 antisense, demonstrating that cyclin D1 is a critical downstream target of Neu-induced transformation (1). Cyclin D1 protein is increased in abundance in mammary tumors induced by overexpression of wild-type Neu or activating mutants of Neu in transgenic mice. Overexpression of transforming mutants of Neu (NeuT) induced cyclin D1 expression and promoter activity in MCF7 cells through an extracellular signal-related kinase but not PI3K/Akt signaling pathways. Cyclin D1 transcriptional induction by NeuT required E2F and Sp1 DNA binding sites in the cyclin D1 promoter (1). Cyclin D1 is required for terminal alveolar breast bud development in the mouse, and substantial morphological differences are observed in the mouse gland of D1 homozygote knock-out mice. In recent studies, Moloney murine tumor virus-Erb-B2 transgenic mice tumorigenesis was abrogated in mice homozygously deleted for the *cyclin D1* gene, suggesting a critical role for cyclin D1 in mammary gland development and tumorigenesis (23).

Flavopiridol is a flavanoid derived from rohitukine, which is a potent nonspecific inhibitor of cyclin-Cdk and an active anticancer agent (IC_{50}, ~100 nM; Refs. 24–31). On the basis of equally impressive activity in human tumor xenograft models, flavopiridol has entered the clinic and has shown antitumor activity in patients with advanced cancer (32–34). The mechanism responsible for cell cycle arrest remains to be determined. Because cyclin D1 encodes a rate-limiting function in the G_1 phase transition in breast cancer cells (35, 36), the reduction in cyclin D1 may play an important role in the cell cycle arrest properties of flavopiridol. There is selective early depletion of cyclin D1 in MCF7 cells exposed to flavopiridol within 3 h. Subsequently, cyclin D3 levels decrease without alteration in cyclin D2, G, or E (37). It has been demonstrated that the reduction in cyclin D1 protein and mRNA is a consequence of a specific decline in cyclin D1 promoter activity (37).

In this report, we describe the combined use of trastuzumab (a monoclonal antibody targeting the Neu receptor that reduces its activation and the activation of the Ras-MAPK pathway) and flavopiridol (which inhibits cyclin-Cdk activity directly) in two Neu-overexpressing human breast cancer cell lines. The current studies demonstrate synergy with combination drug therapy and suggest that the combination of trastuzumab and flavopiridol synergistically inhibit the Ras-MAPK and/or PI3K/Akt pathway, which is associated with reduced abundance of cyclin D1 and/or Cdks and decreased S-phase progression.

Materials and Methods

Materials. Flavopiridol was provided by Drs. Edward Sausville and Robert J. Schultz (Drug Synthesis and Chemistry Branch, Developmental Therapeutics Program, Division of Cancer Treatment and Diagnosis, National Cancer Institute) and pharmacy grade trastuzumab (Herceptin) was from Genentech (San Francisco, CA). Stock concentrations of flavopiridol (1000-fold) were prepared in DMSO and stored at −20°C before use. Trastuzumab was purchased from commercial sources in vials each containing 440 mg of trastuzumab, 9.9 mg of L-histidine HCl, 6.4 mg of L-histidine, 400 mg of α,α-trehalose dihydrate, and 1.8 mg of polysorbate 20, USP. Each vial was reconstituted with 20 ml of supplied Bacteriostatic Water for Injection, USP, containing 1.1% benzyl alcohol as preservative. The final trastuzumab solution strength per vial was 21 mg/ml (~140 μM) at pH 6.01–6.07. Trastuzumab control or vehicle was prepared with 9.9 mg of L-histidine HCl, 6.4 mg of L-histidine, 400 mg of α,α-trehalose dihydrate, and 1.8 mg of polysorbate 20, USP in 20 ml of supplied Bacteriostatic Water for Injection, USP, containing 1.1% benzyl alcohol as preservative.

Cell Cultures. All cell lines used in this study were purchased from the American Type Culture Collection. Cells were maintained at 37°C in 5% CO_2 in a humidified incubator. Human breast cancer cell lines (MCF7, MDA-MB-453, MDA-MB-231, and HBL-100) were cultured in DMEM (Life Technologies, Inc., Grand Island, NY) supplemented with 10% (v/v) FBS. Human breast cancer cell lines (SKBR3, BT-474, and BT-483) were cultured in RPMI 1640 (Life Technologies, Inc.) supplemented with 10% FBS and 2 mM glutamine. T-47D breast cancer cells were cultured in RPMI 1640 supplemented with human insulin at 10 μg/ml (CSL-Novo, North Rocks, New South Wales, Australia) and 10% FCS (36).

Analysis of Single and Combined Drug Effects. Aliquots of 5×10^3 SKBR3 cells or BT-474 cells/well were plated in 96-well microdilution plates, respectively. The MDMBA-453, BT-483, MDA-MB-231, and HBL-100 cells were assayed in a similar manner. In separate experiments, after a ~12-h adherence to the plate after seeding, the cells were treated with serial dilutions of each drug alone and with both drugs given simultaneously at a flavopiridol:trastuzumab ratio corresponding to 25:1 or 50:1. After incubation for 68 h, each well was subsequently stained with 20 μl of PMS CellTiter 96 AQ_{ueous} One Solution Reagent (CellTiter 96 AQ_{ueous} Non-Radioactive Cell Proliferation Assay kit; Promega Corp., Madison, WI). After 4 h incubation, the plates were analyzed by an ELISA reader at a wavelength of 490 nm. Absorbance at this wavelength correlates with survival ($r = 0.997$). The absorbance values from the control wells on each plate were compared to ensure even loading of cells from plate to plate in a given experiment and from experiment to experiment. Multiple drug effect analysis was performed using a computer software program, CalcuSyn (Biosoft, Cambridge, United Kingdom; Ref. 38–40). Fractional survival (*f* or *fa*) was calculated by dividing the absorbance value at 490 nm in the treated plates by the 490 nm absorbance values obtained from the control plates. Log [(1/f) − 1] was plotted against log (drug dose). From the resulting median effect lines, the X-intercept (log IC_{50}) and slope *m* were calculated for each drug and also for the combination of trastuzumab plus flavopiridol by the method of least squares. These parameters were then used to calculate doses of the individual drugs as well as for the combination that would yield a range of f

values (0.95, 0.90, 0.85, ... 0.05) and CombI according to equations described in the CalcuSyn software manual (38–40). For drugs that are mutually nonexclusive in terms of having independent modes of action ($a = 1$); CombI <1, $= 1$, and >1 indicates synergism, additive effect, and antagonism, respectively. The Student t test was applied to the mean CombI values resulting from separate multiple experiments at the multiple effect level to test for significance of the CombI values diverging from CombI $= 1$. For the PD 98059 (selective MEK1 inhibitor; Ref. 41) and LY 294002 (selective PI3K inhibitor; Ref. 42) combination studies with flavopiridol conducted using SKBR3 cells, respectively, the fixed LY 294002 concentrations tested were 6.25, 12.5, and 25 μM, and the fixed PD 98059 concentrations were 12.5, 25, and 50 μM. For SKBR3 cells, PD98059 concentrations $\geq$50 μM result in complete inhibition of MAPK signaling, and LY 294002 $\geq$10 μM also results in complete inhibition of PI3K signaling (42).

Transfection Assays. T-47D cells expressing human cyclin D1 under the control of a zinc-responsive metallothionein promoter (T-47D ΔMTcycD1) as well as mock (vector alone)-transfected cells (T-47D ΔMT) were a kind gift from Dr. Robert L. Sutherland (St. Vincents Hospital, Sydney, New South Wales, Australia; Ref. 36). SKBR3 cells in log exponential phase of growth were cotransfected with CD20 plasmid and pcz-cyclin D1 construct (43, 44). Twenty-four h after cotransfection, cells were treated with flavopiridol, trastuzumab, or both. After incubating cells with drug(s) for 72 h, cells were stained with CD20 antibody and then prepared for cell cycle analysis (44).

Clonogenic Assays. 5×10^3 cells per well were seeded in 6-well plates using RPMI 1640 with 1% FBS. After 24 h of growth at 37°C, cells were treated at different doses of flavopiridol, trastuzumab, or flavopiridol and trastuzumab. After 10 days incubation with drug(s) or control medium, the cells were washed with PBS solution twice, fixed in 10% acetic acid for 10 min, then stained with crystal violet for 10 min, and finally rinsed with distilled water at room temperature. The colonies ($>$50 μm) were then visually counted in randomly chosen 1-mm $\times$ 1-mm grid repeated three times. Statistical analyses of the mean number of colonies were performed by using the Mann-Whitney t test, with significant differences established as $P < 0.05$.

Cell Cycle Analysis. Analysis of cell cycle effects were performed as described previously (19, 45). Cells were collected in PBS, fixed in 70% ethanol at 4°C to permeabilize the cells, and incubated for 5 min in citrate buffer (750 mM Na_2HPO_4, 750 μM sodium citrate, pH 7.8). The cells were resuspended in 1 ml PBS containing 20 μg/ml propidium iodide (Sigma) plus 5 units of RNase A (Sigma) and incubated for 30 min at room temperature. Flow cytometric analyses were carried out in a fluorescence-activated sorter (FACStar plus; Becton Dickinson) with a 360 nM Argon-Iron laser. Analysis of cell cycle (44) and measurements of subdiploid ($<$2N) DNA content of propidium iodide-stained nuclei was performed as published previously (46).

Western Blot Analysis. The relative abundance of each specific protein in 50 μg of whole cell lysate was determined by Western analysis as described previously (19, 45, 47, 48).

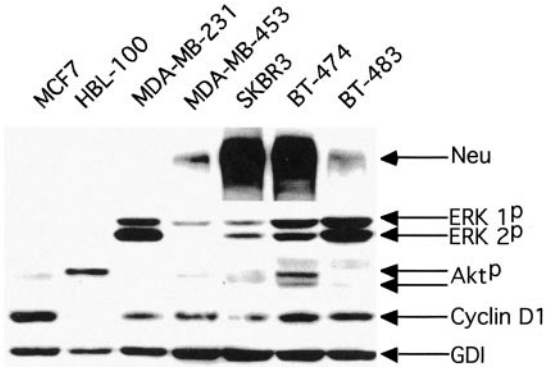

Fig. 1. Expression levels of Neu, activated ERK, and Akt in a panel of human breast cancer cell lines. Lysates from human breast cancer cell lines MCF7, HBL-100, MD-MBA-231, MD-MBA-453, SKBR3, BT-474, and BT-483 were tested on Western blots with antibodies to Neu; phosphorylated ERK1, ERK2, and Akt; and cyclin D1. Membranes were reprobed for GDI abundance to normalize lanes for protein content.

The following antibodies were used: polyclonal anti-Neu (AB-1; Oncogene); polyclonal anti-cyclin D1 (AB-3; Neomarkers); polyclonal anti-RB (AB-2; Oncogene); polyclonal anti-cyclin D1-specific phosphorylated pRB (Ab 169); polyclonal anti-cdc25A (Ab 144; Santa Cruz Biotechnology); polyclonal anti-Cdk4 (C-22; Santa Cruz Biotechnology); polyclonal anti-Cdk2 (H-298; Santa Cruz Biotechnology); polyclonal anti-MEK1 (12B; Santa Cruz Biotechnology); monoclonal phospho-specific MEK-3/6 antibody (B9; Santa Cruz Biotechnology); polyclonal anti-glycogen synthase kinase 3β (H76; Santa Cruz Biotechnology); polyclonal anti-Shc (C20; Santa Cruz, Biotechnology); polyclonal anti-AKT and anti-phospho (Ser-473) specific AKT (Signal Transduction); polyclonal anti-ERK1/ERK2 and monoclonal anti-phospho ERK (Santa Cruz Biotechnology); monoclonal anti-phospho-JNK (G-7; Santa Cruz Biotechnology); monoclonal anti-FLAG antibody (Sigma); and polyclonal anti-GDI (a gift from Dr. Perry Bickel, Washington University, St. Louis, MO; Ref. 49) as loading control. Each blot was repeated at least twice under a minimum of three exposure times and reprobed with polyclonal antibody to GDI for protein content normalization. Selected bands on films were optically scanned and quantitated by ImageQuant software analysis (Molecular Dynamics) and the remaining by visual inspection.

Results

SKBR3 and BT-474 Cells Overexpress Neu Protein and Have an Active MAPK and PI3K Signaling Pathway. Breast cancer cells in exponential growth, MCF7, HBL-100, MDA-MB-231, MDA-MB-453, BT-474, BT-483, and SKBR3, were assayed for Neu protein abundance and activity of the MAPK and PI3K pathway. SKBR3 and BT-474 cells showed the highest levels of Neu and an active ERK pathway (Fig. 1). The effects of trastuzumab and flavopiridol on cellular proliferation using the MTS assay were assessed in SKBR3 and BT-474 cells as these lines overexpress Neu and express an active MAPK pathway. Both SKBR3 and BT-474 cells also have an active PI3K/Akt pathway; however, there was weaker activation of Akt in SKBR3 cells when compared with BT-474 cells. In contrast, MCF7, HBL-100, MD-MBA-231,

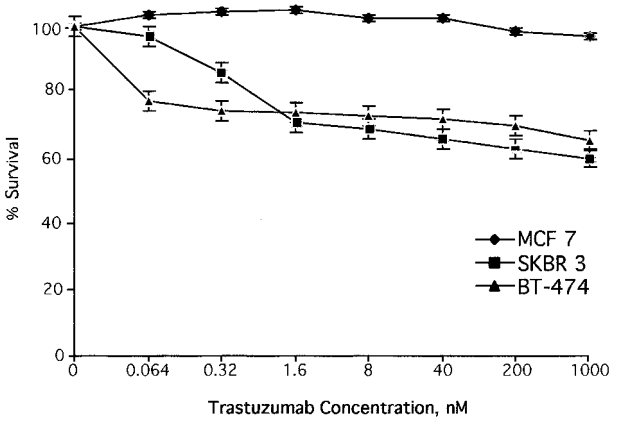

Fig. 2. Survival (growth) curves in MCF7, SKBR3, and BT-474 cells using various concentrations of exposure to trastuzumab for 72 h. These cell lines were treated with various concentrations of trastuzumab or control vehicle for 72 h, following which the cells were subject to the MTS assay (CellTiter 96 AQ_{ueous} Non-Radioactive Cell Proliferation Assay kit; Promega). *Bars,* SE.

MD-MBA-453, and BT-483 cells have significantly lower abundance of Neu compared with SKBR3 or BT-474 cells. Although the MAPK pathway was more active in MDA-MBA-231 and BT-483 cells compared with that in BT-474 cells, both cell lines have a minimally active PI3K/Akt pathway. MD-MBA-231, MD-MBA-453, and SKBR3 cell lines express and have relatively equal abundance of cyclin D1 protein. Compared with SKBR3, MCF7, BT-474, and BT-483 have higher levels of cyclin D1, and HBL-100 has lower abundance of cyclin D1 (Fig. 1).

The Effects of Trastuzumab and Flavopiridol on SKBR3 and BT-474 Cell Proliferation and Survival. SKBR3, BT-474, and MCF7 cells were treated with increasing concentrations of trastuzumab or control vehicle for 72 h to determine the effects on cellular proliferation. There was a significant reduction (30–40%) in proliferation of SKBR3 cells exposed to trastuzumab concentrations between 1.6 and 1000 nM. At these concentrations, there was no significant effect on the survival of MCF7 cells (Fig. 2). BT-474 cells were slightly more sensitive to low concentrations of trastuzumab (≥0.064 nM); however, the maximum survival fraction was the same as in SKBR3 cells.

When SKBR3 cells were treated with trastuzumab (*T*) and flavopiridol (*F*) simultaneously for 72 h, cytotoxic synergism was observed (flavopiridol alone IC_{50} ~110 nM *versus* $F + T$ IC_{50} ~90 nM). The flavopiridol dose-response curve was shifted to the left with combination treatment. This effect is depicted in the summary graph as a decrease in the flavopiridol IC_{50} and CombI <1 when the two agents are administered simultaneously at a fixed trastuzumab dose of 200 nM (data not shown) or fixed ratio of 25:1 (Table 1 and Figs. 3 and 4). For SKBR3 cells, the CombI values remain <1 for effective doses of both drugs that would inhibit up to 75% of cells, implying cytotoxic synergy. At ED_{90} doses, where 90% of the cells are affected by flavopiridol, the CombI values exceed 1, suggesting no effect or antagonism. Note that the linear regression correlation coefficient (*r* values >0.9) of the median effect plots reflect that the dose-effect relationships of the drugs conform to the principle of mass action (Table 1). Similar synergism was observed with fixed ratio flavopiridol (*F*) to trastuzumab (*T*) of 50:1 (data not shown). For BT-474 cells, there was a similar shift in IC_{50} (flavopiridol alone IC_{50} ~140 nM *versus* $F + T$ IC_{50} ~90 nM; Fig. 3). At a fixed flavopiridol to trastuzumab ratio of 25:1, more striking synergism (CombI <1) was observed over the entire concentration range (multiple effect levels, *Fa*) tested. This effect is depicted in summary Table 2 and graph (Fig. 4) because CombI values remain <1 for effective doses of both drugs that inhibit up to 90% of cells, implying cytotoxic synergy. For BT-474, similar synergism is observed with fixed ratio flavopiridol (*F*):trastuzumab (*T*) of 50:1 or using a fixed concentration of trastuzumab of 200 nM with various concentrations of flavopiridol (data not shown).

To evaluate sequence dependency of both drugs given in combination with respect to cytotoxic synergy, SKBR3 cells were treated with flavopiridol for an initial 12 h, followed by addition of trastuzumab for 72 h; this was also done in reverse with trastuzumab treatment for an initial 12 h followed by addition of flavopiridol for 72 h. For both experiments, performed simultaneously, a fixed ratio of flavopiridol: trastuzumab of 50:1 was chosen. Synergy determined as CombI <1 was observed independent of sequence of administration of the drugs. The lowest CombI values, however, were observed with the schedule of flavopiridol followed by trastuzumab treatment (data not shown). Combination drug cytotoxic synergy using the MTS assay was not observed in MCF7 (low Neu; relatively inactive Ras-MAPK-Akt pathway), HBL-100 (low Neu; active Akt pathway), MDA-MB-231 (low Neu; active MAPK pathway), BT-483 (intermediate Neu levels; active MAPK pathway), and MDA-MB-453 cells (intermediate Neu levels; low to moderate MAPK-Akt pathway activity; Fig. 1 and data not shown).

The Effects of Trastuzumab and Flavopiridol on Contact-dependent SKBR3 and BT-474 Cell Growth Using Clonogenic Assays. To determine the effect of trastuzumab and flavopiridol on contact-dependent growth, colony formation assays were performed. In contact-dependent growth assay, the colony formation of SKBR3 cells was reduced to ~55% of control value with 50 nM of flavopiridol alone. Colony formation was reduced to 35% of control value with 2 nM of trastuzumab alone; however, colony formation was reduced to ~20% of control value when trastuzumab (2 nM) was combined with flavopiridol (50 nM; $P < 0.05$; Fig. 5). To assess the sequence effect of drug treatment, SKBR3 cells were initially treated with trastuzumab and 12 h later followed by flavopiridol or in reverse sequence. Similar synergy in inhibition of colony formation was demonstrated when agents were added in either sequence (data not shown). In comparison to drug effects on SKBR3 colony formation, similar results were obtained with BT-474 cells (Fig. 5). Colony formation of BT-474 cells was reduced to ~43% of control with the addition of 50 nM flavopiridol alone. Colony formation was reduced to ~28% with the addition of 2 nM trastuzumab alone; however, colony formation was reduced to ~20% of control value with combination treatment as compared with cells treated with equivalent con-

Table 1 Summary table of the CombCI values at 50–90% effective doses (ED) of flavopiridol + trastuzumab in SKBR3 cells

In this analysis *Fa* and *Fu* are the fraction of cells affected or unaffected, respectively, by the dose (*D*) of either drug or antibody. *Dm* is the dose required to produce the median effect (analogous to the IC_{50}), and *m* is the Hill coefficient used to determine whether the dose-response relationship follows a sigmoidal plot (40). Linear regression correlation coefficient (*r* values) of the median effect plots reflect that the dose-effect relationships of the drugs conform to the principle of mass action ($r > 0.9$ validate this methodology; Ref. 38).

Drug(s)	CombCI values at					
	ED_{50}	ED_{75}	ED_{90}	*Dm*	*m*	*r*
Flavopiridol plus Trastuzumab	0.49984	0.91182	1.66335	104.18563 nM	0.84719	0.96
Flavopiridol	NA[a]	NA	NA	NA	1.57933	0.98
Trastuzumab	NA	NA	NA	2.2789e + 006 nM	0.10065	0.99

[a] NA, not applicable.

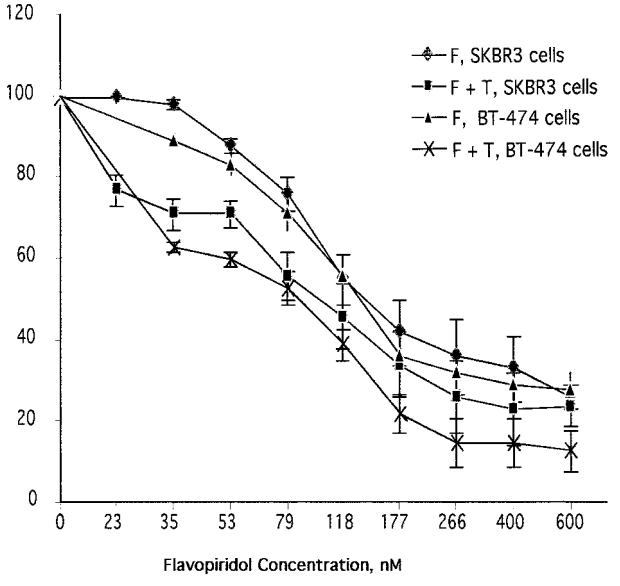

Figs. 3. Survival (Growth) curves in SKBR3 and BT-474 cells treated with flavopiridol (*F*; *T* = 0 nM) or flavopiridol in combination with fixed ratio trastuzumab (*T*; 25:1). Cell treatment details have been described in "Materials and Methods."

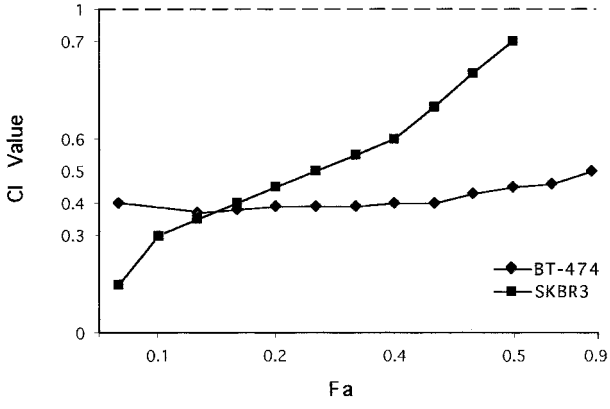

Fig. 4. CombI values for flavopiridol (*F*) in combination with trastuzumab (*T*) at multiple effect levels. CombI values <1 indicate synergy. CombI values for flavopiridol (*F*) in combination with trastuzumab (*T*) at multiple effect levels are shown. *Fa,* the fraction of BT-474 cells and SKBR3 cells affected by the drug (not to scale). CombI values <1 indicate synergy. Multiple drug effect analysis was performed using a computer software program, CalcuSyn (Biosoft; Refs. 35–37). Fractional survival (*f* or *fa*) was calculated by dividing the absorbance value at 490 nm in the treated plates by the 490 nm absorbance values obtained from the control plates. Log [(1/*f*) − 1] was plotted against log (drug dose). From the resulting median effect lines, the X-intercept (log IC_{50}) and slope *m* were calculated for each drug and also for the combination of trastuzumab plus flavopiridol by the method of least squares. These parameters were then used to calculate doses of the individual drugs as well as for the combination that would yield a range of f values (0.95, 0.90, 0.85, ... 0.05) according to equation described in "Materials and Methods." For each level of cytotoxicity, a CombI was generated using an equation based on each drug concentration yielding a combined fractional effect (*f*) as described in "Materials and Methods." For drugs that are mutually nonexclusive in terms of having independent modes of action (*a* = 1); CombI <1, = 1, and >1 indicates synergism, additive effect, and antagonism, respectively. The Student *t* test was applied to the mean CombI values resulting from separate multiple experiments at the multiple effect level to test for significance of the CombI values diverging from CombI = 1.

centrations of single drugs ($P < 0.05$; Fig. 5). These results are consistent with additive cytotoxic effects.

Effect of Cyclin D1 on Trastuzumab- or Flavopiridol-induced Changes on Contact-dependent T-47D Breast Cancer Cell Growth Using Clonogenic Assays. To determine the effect of cyclin D1 on trastuzumab- or flavopiridol-induced growth arrest in T-47D breast cancer cells, colony formation assays were performed using cells previously generated expressing cyclin D1 under the control of a Zn^{2+}-inducible truncated human metallothionein IIA promoter lacking steroid-responsive sequences, designated T-47D ΔMTcycD1 and cells transfected with vector alone, T-47D ΔMT (Ref. 36; Fig. 6*a*). In clonogenic assay, the T-47D ΔMTcycD1 cells treated with flavopiridol at 100 nM, colony formation was reduced to ~90% (±4% SE) of its control; however, colony formation was reduced to ~52% (±4% SE) of control in T-47D ΔMT cells treated with 100 nM flavopiridol alone (Fig. 6*b*). Similarly, colony formation was unaffected in T-47D ΔMTcycD1 cells treated with 4 nM trastuzumab alone compared with its control; however, with the same concentration of trastuzumab, colony formation was reduced to ~82% of control in T-47D ΔMT cells. Colony formation was reduced to ~28% of control value in T-47D ΔMTcycD1 cells treated with 100 nM flavopiridol and 4 nM trastuzumab, whereas in T-47D ΔMT cells treated with the same combination of drugs, colony formation was only reduced to ~17% of its control (Fig. 6*b*). These results are consistent with the inhibitory effects of cyclin D1 on T-47D cell death under selection with flavopiridol, trastuzumab, or a combination of both drugs.

Table 2 Summary table of the CombI values at 50–90% effective doses (ED) of flavopiridol + trastuzumab in BT-474 cells

In this analysis, *Fa* and *Fu* are the fraction of cells affected or unaffected, respectively, by the dose (*D*) of either drug or antibody. *Dm* is the dose required to produce the median effect (analogous to the IC_{50}), and *m* is the Hill coefficient used to determine whether the dose-response relationship follows a sigmoidal plot (40). Linear regression correlation coefficient (*r* values) of the median effect plots (Table 1) reflect that the dose-effect relationships of the drugs conform to the principle of mass action ($r > 0.9$ validate this methodology; Ref. 38).

Drug(s)	CombI values at					
	ED_{50}	ED_{75}	ED_{90}	*Dm*	*m*	*r*
Flavopiridol plus Trastuzumab	0.38442	0.45094	0.52897	68.41 nM	1.00170	0.98
Flavopiridol	NA[a]	NA	NA	177.96 nM	1.17229	0.97
Trastuzumab	NA	NA	NA	5.9357e + 007 nM	0.06163	0.99

[a] NA, not applicable.

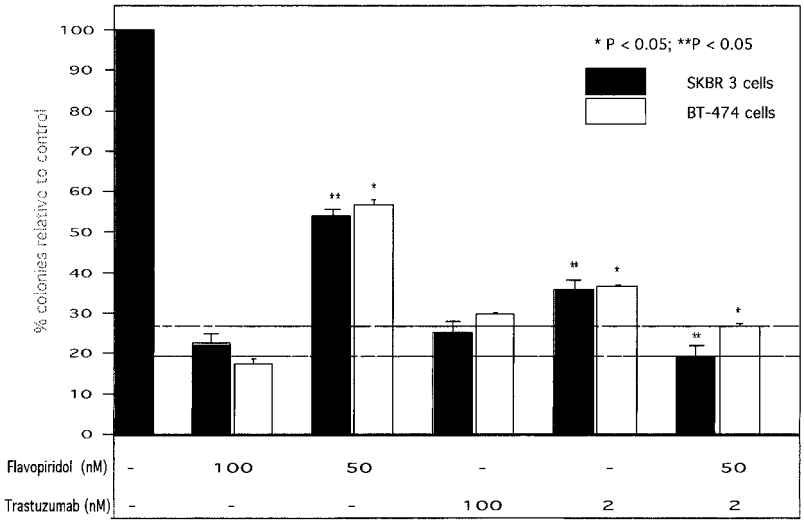

Fig. 5. Synergistic induction of cell death by flavopiridol (*F*) and trastuzumab (*T*). Colony formation assays were carried out as described in "Materials and Methods." Control SKBR3 (■) and BT-474 cells (□) were treated with formulation solvent; with flavopiridol alone at 100 nM; with flavopiridol alone at 50 nM; with trastuzumab at 100 nM; with trastuzumab at 2 nM; and with combination flavopiridol (50 nM) and trastuzumab (2 nM) on days 1–10. The average (*bars,* SE) results of nine independent experiments have been illustrated. There is a significant reduction in colony formation in cells treated with combination drugs as compared with flavopiridol (50 nM) or trastuzumab (2 nM)-treated cells ($P < 0.05$).

Effects of Trastuzumab and Flavopiridol on SKBR3 Cell Cycle. Because the combination of flavopiridol and trastuzumab reduced cell proliferation rates, we performed FACS analysis to determine the effect of each agent on cell cycle distribution (FACStar plus; Becton Dickinson). SKBR3 cells were treated either with trastuzumab or flavopiridol or both agents simultaneously for 24 and 72 h. After 24 h, the S-phase fraction of cells treated with 100 nM flavopiridol alone was 27% ± 3% SE (for control treated cells S-phase fraction ~ 26% ± 2% SE), whereas the S-phase fraction of cells treated with 4 nM trastuzumab alone was 19% ± 1% SE. For flavopiridol plus trastuzumab-treated cells, the S-phase fraction was 15% ± 2% SE. This was accompanied by an increase in cells of similar magnitude in the G_0-G_1 as well as the G_2-M phase of the cell cycle (data not shown). After 72 h, for cells treated with 100 nM flavopiridol, the S-phase fraction was 14% ± 5% SE (compared with control-treated cells, S-phase fraction ~24% ± 1% SE); for cells treated with 4 nM trastuzumab alone, the S-phase fraction was 16% ± 2% SE. For cells treated with flavopiridol and trastuzumab, the S-phase fraction was lower, ~8% ± 2% SE compared with 100 nM flavopiridol-treated or 4 nM trastuzumab-treated cells (data not shown). These results are consistent with inhibitory effects of trastuzumab and flavopiridol on the G_1-S cell cycle boundary.

To determine the effect of cyclin D1 on entry of drug-treated cells into S-phase, we performed FACS analysis of SKBR3 cells transiently cotransfected with a CD20 expression plasmid and pcz-cyclin D1 expression plasmid (pcz-flag D1) as described previously (43, 44). Drug(s) and control-treated CD20 positive (+) and negative (−) cells were selected and analyzed for cell cycle distribution by FACS using propidium iodide staining (46). Cells were cotransfected with pMACS4 and pcz-flag D1, and then MACS sorted express flag-cyclin D1 as shown in Fig. 7*a*. At flavopiridol concentrations of 100 or 200 nM, after 72 h, >85% of CD20+ cells remained in S-phase relative to control-treated CD20+ cells; however, in CD20− cells after 72 h, <50% of cells remained in S-phase relative to control-treated CD20− cells (Fig. 8). Similarly, 100 nM trastuzumab reduced the percentage of S-phase cells to ~45% of control value in CD20− cells; however, the same concentration of trastuzumab reduced the percentage of S-phase cells to ~15% of control value in CD20+ cells. A similar reduction profile is seen in CD20− and CD20+ cells treated with 4 nM trastuzumab (Fig. 7*b*). These data suggest that in transient transfection experiments, cyclin D1 expression inhibits drug-induced reduction in S-phase SKBR 3 cells and complements findings of inhibitory effects of cyclin D1 on T-47D cell death under selection

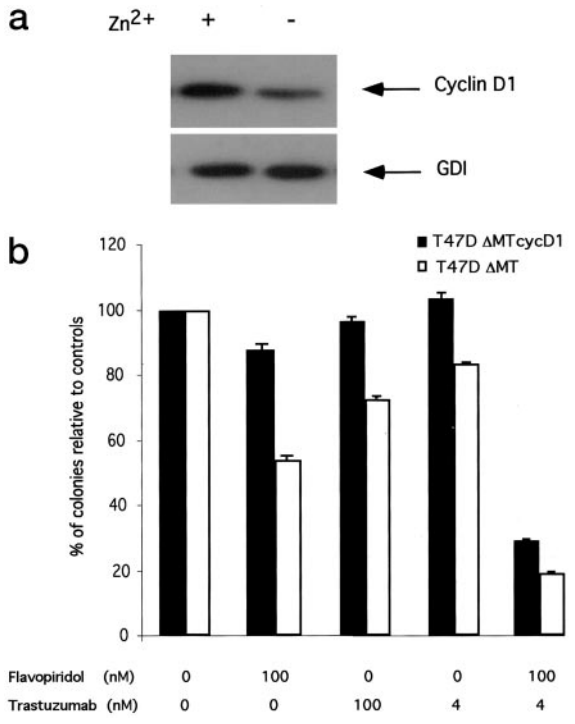

Fig. 6. *a,* induction of cyclin D1 expression in T-47D ΔMTcycD1 stable cells with Zn^{2+} as published previously (36). Lysates from human breast cancer cell lines T-47D ΔMTcycD1 exposed to 50 μM $ZnSO_4$ (+) or no $ZnSO_4$ (−) were tested on Western blots with antibodies to cyclin D1. Membranes were reprobed for GDI abundance to normalize lanes for protein content. *b,* effect of flavopiridol and/or trastuzumab on T-47D ΔMTcycD1 and T-47D ΔMT cells. Colony formation assays were carried out as described in "Materials and Methods." T-47D ΔMTcycD1 cells (■) and T-47D ΔMT (□) were treated with formulation solvent; with flavopiridol alone at 100 nM; or trastuzumab at 100 nM or 4 nM; or flavopiridol (50 nM) and trastuzumab (2 nM) on days 2–10. After plating cells on day 1 in the presence of Zn^{2+} as published previously (43), cells were subsequently exposed to drug(s) as indicated. The average (*bars,* SE) results of three independent experiments have been illustrated.

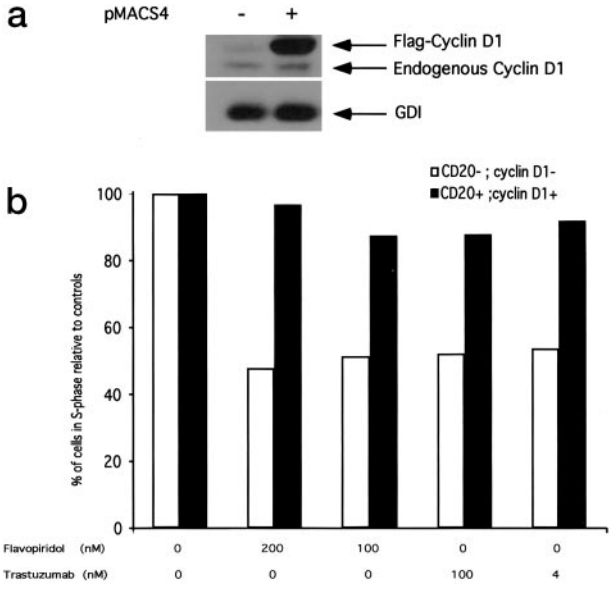

Fig. 7. *a,* SKBR3 cells cotransfected pcz-flag D1 and pMACS4 using a technique published previously (43, 44) show expression of flag-cyclin D1 protein by Western blot. pMACS4 sorted lane is marked (+), and pMACS4 negative lane is marked (−). pMACS4 + and − cells were collected and lysed for total protein and subjected to Western blot analysis for cyclin D1 protein using anti-cyclin D1 antibody (see "Materials and Methods"). Membranes were reprobed for GDI to normalize lanes for protein content. *b,* cell cycle analysis of cyclin D1-transfected SKBR3 cells. SKBR3 cells transfected with pcz-cyclin D1 and CD20 were treated with drugs as indicated. CD20+ (■) and CD20− (□) selected cell cycle phase distribution after treatment with flavopiridol or trastuzumab as shown. Each *column* represents the percentage of cells in S-phase as a fraction of its percentage of control cells in S-phase. The controls have been normalized to 100%. The data are means of two separate experiments.

with flavopiridol, trastuzumab, or a combination of both drugs.

Effects of Trastuzumab and Flavopiridol Treatment of SKBR3 Cells on Cyclin D1 and pRB. Western blots to assess cyclin D1 and pRB were performed using SKBR3 cell lysates exposed to no drug treatment, flavopiridol, trastuzumab, or the combination of flavopiridol and trastuzumab administered simultaneously for 72 h (Fig. 8). Single-agent flavopiridol at concentrations of 100 and 150 nM showed a 49 and ~90% decrease in cyclin D1 protein abundance compared with control cells, respectively. Cells treated with 50 nM flavopiridol did not show a significant change in cyclin D1 abundance compared with control-treated cells (95% abundance level compared with control). Cells treated with trastuzumab (4 nM) and flavopiridol (100 nM) showed a ~90% reduction in cyclin D1 protein when compared with flavopiridol (100 nM)-treated cells (Fig. 8).

Similarly, flavopiridol decreases in Cdk4 abundance at concentrations >50 nM. Trastuzumab-treated cells (100 or 4 nM) also show reduced Cdk4 abundance when compared with control-treated cells. The combination of 100 nM flavopiridol and 4 nM trastuzumab reduced Cdk4 abundance when compared with equivalent concentrations of either agent alone. In contrast, however, the combination of 50 nM flavopiridol and 2 nM trastuzumab resulted in an increase in Cdk4 abundance compared with cells treated with 4 nM trastuzumab (Fig. 8). Flavopiridol-treated cells also showed a dose-dependent decrease in Cdk2 abundance. Cells treated with 100 or 4 nM trastuzumab also showed reduced Cdk2 abundance when compared with control-treated cells. The combination of 100 nM flavopiridol and 4 nM trastuzumab reduced Cdk2 abundance when compared with cells treated with 100 nM flavopiridol alone (Fig. 8). Furthermore, there was a ~2-fold reduction in Cdk2 abundance compared with cells treated with 4 nM trastuzumab alone. The combination of 50 nM flavopiridol and 2 nM trastuzumab reduced Cdk2 abundance when compared with cells treated with 50 nM flavopiridol alone. The abundance of Cdk2 in cells treated with 50 nM flavopiridol plus 2 nM trastuzumab was nearly equivalent to cells treated with 100 nM flavopiridol and 4 nM trastuzumab (Fig. 8).

The reduction in cyclin D1 is paralleled by a similar decrease in the abundance of phosphorylated pRB using an antibody that recognizes cyclin D1-Cdk4-dependent Ser-795 pRB phosphorylation (Fig. 8). In comparison with flavopiridol effects on cyclin D1, Cdk4, and Cdk2 abundance, flavopiridol-treated cells showed a dose-dependent de-

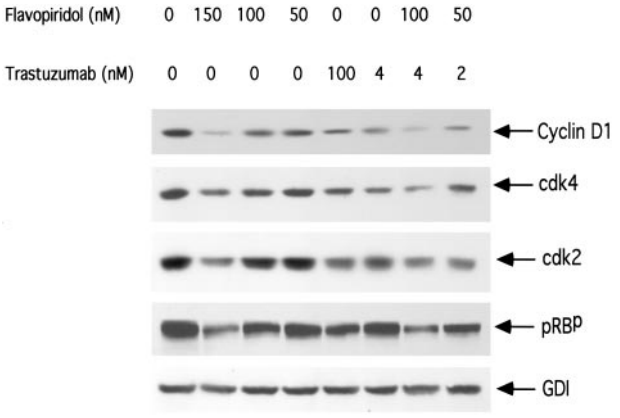

Fig. 8. Lysates from human breast cancer cell line (SKBR3) that were exposed to flavopiridol (100 or 200 nM), trastuzumab (4 or 100 nM), or both were tested on Western blots with antibodies to cyclin D1, Cdk4, Cdk2, and phosphorylated pRB. Membranes were reprobed for GDI to normalize lanes for protein content.

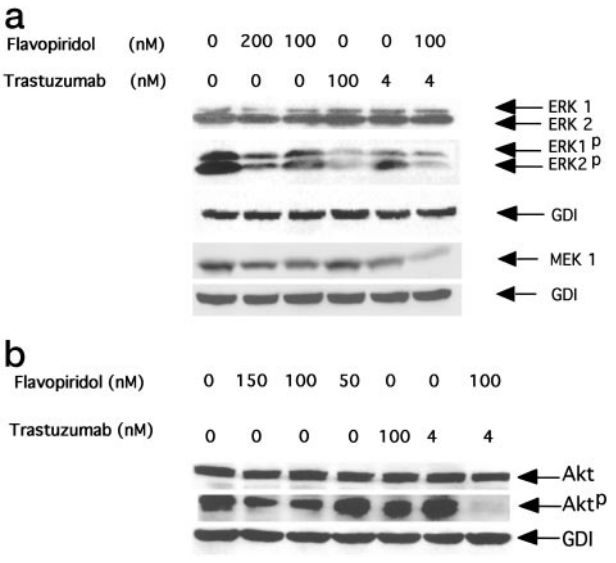

Fig. 9. *a,* lysates from human breast cancer cell line (SKBR3) that were exposed to flavopiridol (100 or 200 nM), trastuzumab (4 or 100 nM) or both were tested on Western blots with antibodies to ERK1, ERK2, and MEK 1. Membranes were reprobed for GDI to normalize lanes for protein content. *b,* lysates from human breast cancer cell line (SKBR3) that were exposed to various concentrations of flavopiridol, trastuzumab, or both were tested on Western blots with antibodies to Akt and phosphorylated Akt (Akt^P). Membranes were reprobed for GDI to normalize lanes for protein content.

crease in pRB phosphorylation. Cells treated with 100 or 4 nM trastuzumab also showed reduced pRB phosphorylation as compared with control-treated cells. The combination treatment of cells with 100 nM flavopiridol and 4 nM trastuzumab resulted in >85% reduction in phosphorylated pRB when compared with 4 nM trastuzumab and a >60% reduction when compared with cells treated with 100 nM flavopiridol alone. There was a similar decrease (by ~50%) in phosphorylated pRB at lower concentrations of the combination of flavopiridol (50 nM) and trastuzumab (2 nM) when compared with cells treated with 50 nM flavopiridol alone. In separate Western blots, total pRB levels remain unchanged across increasing flavopiridol and trastuzumab concentrations; however, phosphorylated pRB as evaluated using a polyclonal anti-RB antibody (AB-2; Oncogene) showed a similar decrease in total cell cellular phosphorylated pRB (data not shown). There is no observed difference in the abundance of cdc25A phosphatase in control-treated and drug-treated cells (data not shown).

Effects of Trastuzumab and Flavopiridol Treatment on SKBR3 ERK Pathway. We performed Western blots to determine the expression and activity profile of MAPK isoforms that are involved in Neu signaling. The abundance of total ERK1 and ERK2 remained unchanged in cells treated with flavopiridol, trastuzumab, or the combination of both drugs given simultaneously for 72 h as compared with control-treated cells. Cells treated with flavopiridol 100 nM showed slightly reduced ERK activity as measured by an antibody directed against phosphorylated ERK1 and ERK2 as compared with control-treated cells. Cells exposed to 200 nM flavopiridol showed a reduction in phosphorylated ERK1 and ERK2 when compared with cells treated with 100 nM flavopiridol. Cells treated with 100 nM trastuzumab showed negligible levels of phosphorylated ERK1 and ERK2; however, cells treated with 4 nM trastuzumab showed a >70% reduction in phosphorylated ERK1 and ERK2. There was a ~40% reduction in the abundance of activated ERK1 and ERK2 (phosphorylated ERK1 and ERK2) in cells treated with the combination of trastuzumab (4 nM) and flavopiridol (100 nM) when compared with abundance in cells treated with 100 nM flavopiridol (Fig. 9*a*).

To examine the effects of our drugs on stress-induced signaling proteins, we performed Western blots to determine the protein abundance of total JNK 1 and activated JNK. Total JNK 1 abundance remained unchanged in cells treated with flavopiridol, trastuzumab, or flavopiriol plus trastuzumab given simultaneously for 72 h as compared with control-treated cells. Flavopiridol (100 nM)-treated cells showed increased JNK 1 activity as compared with control-treated cells when measured as increased phosphorylated JNK 1 abundance using an monoclonal antibody that recognizes phosphorylated JNK (G-7; Santa Cruz Biotechnology). There was a ~40% reduction in the abundance of activated JNK, whereas there was no change in total JNK 1 protein abundance with 100 nM flavopiridol and 4 nM trastuzumab compared with 100 nM flavopiridol-alone treated cells (data not shown). However, the abundance of phosphorylated JNK 1 is nearly the same for cells treated with combination 100 nM flavopiridol plus 4 nM trastuzumab *versus* control-treated or cells treated with 4 nM trastuzumab.

To examine another component of the stress-activated signaling pathway and effects of our drugs on this protein, we performed Western blots to determine protein abundance of total p38 (HOG) and activated (phosphorylated) p38 (data not shown). The abundance of total p38 remains unchanged with drug (flavopiridol, trastuzumab, or combination flavopiridol plus trastuzumab) treatment when compared with control-treated cells. Cells treated with 100 nM flavopiridol showed a reduction in phosphorylated p38 as compared

with control-treated cells; however, in comparison to this, cells treated with 4 nM trastuzumab alone showed a marked reduction (>95%) in the abundance of phosphorylated p38. Cells treated with 100 nM flavopiridol plus 4 nM trastuzumab showed no significant change in the abundance of phosphorylated p38 when compared with its abundance in cells treated with 4 nM trastuzumab alone. JNK abundance and activity as well as p38 abundance and activity did not change with combination treatment when compared with equivalent concentrations of trastuzumab alone (data not shown). These findings suggest that combination treatment with flavopiridol and trastuzumab does not significantly alter the stress-activated MAPK pathway.

To examine the effects of our drugs on other Ras-MAPK and stress-induced signaling proteins, we performed Western blots to determine the protein abundance of phosphorylated MEK 3/6 (data not shown) and total MEK 1 (Fig. 9*a*). There was no change in the abundance of phosphorylated MEK 3/6 in cells treated with flavopiridol, trastuzumab, or the combination of flavopiridol and trastuzumab when compared with control. Cells treated with 4 nM trastuzumab showed a >30% decrease in MEK 1 abundance compared with cells treated with 100 nM trastuzumab. Cells treated with combination flavopiridol (100 nM) and trastuzumab (4 nM) had decreased MEK 1 abundance by ~85% when compared with cells treated with 4 nM trastuzumab. The reduced amount of MEK 1 protein in cells treated with combination drugs implicates and supports the role of ERK signaling as an important determinant in drug-induced inhibition of cell proliferation. Furthermore, in keeping with the absence of alteration in p38 and JNK, combination drug treatment does not alter the abundance of phosphorylated MEK 3/6, implying that the stress-activated MAPK pathway is not an important determinant in combination drug-induced changes in cellular signal transduction or inhibition of cell proliferation.

Effects of Trastuzumab and Flavopiridol on Abundance and Activity of the PI3K/Akt Pathway. To determine the importance of Akt signaling in SKBR3 cells treated with flavopiridol or trastuzumab or both given simultaneously for 72 h, we performed immunoblots to determine the expression profile of total Akt content and activated (phosphorylated) Akt (Fig. 9*b*). Total Akt abundance was unchanged in cells treated with flavopiridol, trastuzumab, or both drugs compared with control-treated cells. Cells treated with flavopiridol showed a dose-dependent decline in phosphorylated Akt; however, the abundance of phosphorylated Akt in cells treated with 100 and 150 nM flavopiridol was nearly the same. In contrast, cells treated with 4 nM trastuzumab had ~45% more phosphorylated Akt than cells treated with 100 nM trastuzumab. In cells treated with combination drug therapy, there was no change in the abundance of total Akt protein; however, there was a >90% reduction in the abundance of activated (phosphorylated) Akt when compared with phosphorylated Akt abundance in 100 nM flavopiridol-treated or 4 nM trastuzumab-treated cells (Fig. 9*b*).

Effects of Flavopiridol and PD 98059 or LY 294002 on SKBR3 Cell Proliferation and Survival. SKBR3 cells were treated with increasing concentrations of PD 98059 (0–100 μM), LY 294002 (0–50 μM), or control vehicles, respectively, for 72 h to determine the effects on cellular proliferation. There was a small reduction (~20%) in proliferation of SKBR3 cells exposed to 100 μM PD 98059 (data not shown). However, at this concentration PD 98059 completely inhibited MAPK activity in SKBR3 cells (42). When SKBR3 cells were treated with flavopiridol (*F*) and PD 98059 using concentrations up to 50 μM simultaneously for 72 h, no cytotoxic synergism was observed (*F* alone IC_{50} ~200 nM *versus F* + *PD* 98059 IC_{50} ~200 nM; data not shown). The CombI values across *Fa* values ranging from 0.2 to 0.89 were close to or above 1.0. There was a more significant reduction (~90%) in proliferation of SKBR3 cells exposed to 50 μM LY294002 (IC_{50} ~15 μM). When SKBR3 cells were treated with flavopiridol (*F*) and LY 294002 using concentrations up to 25 μM simultaneously for 72 h, cytotoxic synergism was observed with the lowest LY 294002 concentration of 6.25 μM (CombI <1 up to *Fa* <0.9; data not shown), and the synergism increased proportional to increases in the LY 294002 concentration (Fig. 10).

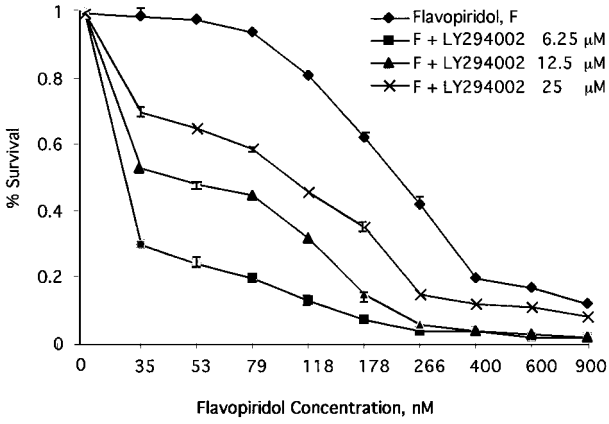

Fig. 10. Survival (growth) curves in SKBR3 cells treated with flavopiridol (*F*; no LY 294002 present) or flavopiridol in combination with increasing concentrations of LY 294002. Cell treatment details have been described in "Materials and Methods."

Discussion

Our results demonstrate that flavopiridol and trastuzumab together have an enhanced effect in their inhibition of cell proliferation, DNA synthesis, and contact-dependent growth in two breast cancer cells lines that overexpress endogenous Neu. We did not observe synergy using the MTS assay for cell lines that had low abundance of endogenous Neu and/or lines that expressed Neu but did not exhibit an active MAPK and/or Akt signaling pathway. In the cell lines SKBR3 and BT-474 that overexpressed Neu and did exhibit an active MAPK-Akt signaling pathway, synergy was demonstrated using the MTS assay and additivity in colony formation. In the MTS assays, synergy (CombI <1) was observed with simultaneous treatment, initial treatment with flavopiridol for 12 h followed by trastuzumab, and initial treatment with trastuzumab for 12 h followed by flavopiridol. There was no evidence suggesting that one schedule is superior to another; however, lower CombI values (or the highest levels of syn-

ergy) were observed with flavopiridol treatment followed by trastuzumab treatment. Cyclin D1 levels diminish with combination treatment in a dose-dependent manner. Because Cdk2 and Cdk4 are also consistently down-regulated in cells treated with combination drugs rather than either drug alone, it is feasible to speculate that total cyclin-Cdk kinase activity may be less, and this is reflected in decreased cyclin-D1 specific pRB phosphorylation seen in cells exposed to combination treatment. We corroborate findings that the intracellular signal transduction pathway involves kinase mediators including p42 and p44 ERKs (50), the stress-activated protein kinases (51), and a wortmannin-sensitive phosphoinositide 3-OH kinase (PI3K) activity (52). Reduced Akt and ERK signaling has been observed with combination treatment of SKBR3 cells. The question as to whether inhibition of Akt or the ras-MAPK pathway leads to observed synergy with the combination remains to be proven; however, synergy experiments with LY 294002 (a PI3K inhibitor) suggest that inhibition of PI3K signaling may be important in the observed synergy with flavopiridol. However, PD 98059, a MEK1 inhibitor, plus flavopiridol does not yield synergy, suggesting that the Ras-MAPK pathway may be less important, at least relative to the Akt pathway, in the observed synergy with flavopiridol. Because dephosphorylation events may occur as a result of enhanced phosphatase activity, we assayed for the abundance of cdc25A phosphatase, which is known to promote S-phase entry through dephosphorylation and activation of cyclin E-Cdk2 and cyclin A-Cdk2 (53–55). There was no change in the abundance of cdc25A protein, as assayed by Western blot in control- and drug-treated cells.

Although we found reduced ERK 1/2 signaling in SKBR3 cells exposed to combination treatment with flavopiridol and trastuzumab, others have reported that ERK signaling is not significantly altered with trastuzumab concentrations of 10 μg/ml ($\sim$67 nM) over a exposure period of 240 min (56). We show reduced ERK activation by $\sim$80% at higher concentrations, $\sim$100 nM, after exposure to trastuzumab over 72 h, whereas at lower concentrations, $\sim$4 nM, there is $\sim$40% change in ERK activation. This variability in result may be attributable to the differences in concentrations used, time course of drug exposure, or differences in SKBR3 clones in these studies. However, in MDA-MB-453 and BT-474 human breast cancer cells, inhibition of erbB receptor family does lead to reduced Akt and MAPK signaling (57). Similarly, using an epidermal growth factor receptor signaling inhibitor, AG-1478, Busse *et al.* (58) show that MAPK signaling is markedly reduced in A431 human breast tumor cells. Although these studies reflect alterations of ERK activity by inhibition of erbB-related family members, the implication may be that ERK activity can be reduced by inhibition of erbB2 alone using trastuzumab but may require longer exposure times and may also be an indirect effect of other pathways affected that interact with MAPK activation. However, the importance of ERK inhibition in the synergy seen with flavopiridol is unclear because we show a lack of synergy with flavopiridol combined with PD 98059, suggesting that ERK inhibition may not be an important signaling change correlating with cell survival.

SKBR3 cells exhibit a constitutively active Ser-473-phosphorylated Akt, which is reduced in abundance with treatment with trastuzumab alone and increased in abundance with the treatment of flavopiridol alone; however, active Ser-473-phosphorylated Akt is nearly eliminated by combined treatment with trastuzumab plus flavopiridol. Our results demonstrate that there is augmented down-regulation of phosphorylated Akt with combination drug treatment, suggesting decreased Akt-induced cell signaling. These findings suggest that Akt inactivation may result in enhanced $p27^{kip1}$ abundance (a known inhibitor of cyclin D1-Cdk4 activity), possibly through mechanisms involving enhanced AFX/Forkhead transcription factor activity (59, 60). Because cyclin D1 abundance is diminished, it is likely that inhibition of Akt may also influence cyclin D1 levels through reduced stimulation of FRAP/mTOR kinase (a mammalian homologue of *Saccharomyces cerevisiae* that targets rapamycin TOR1 and TOR2) activity and repression of cyclin D1 translation initiation (61, 62). The mechanism of enhanced depletion of activated Akt is unclear and may result from the effect of flavopiridol on transcriptional activation of PTEN or an ability to block PI3K activity. This is speculation that requires experimental proof; however, there is some basis for such speculation because flavopiridol has been shown to inhibit other enzymes such as glycogen phosphorylase (63), or bind weakly to proteins such as P-glycoprotein (64), or bind to DNA (65), and/or possess ability to inhibit transcriptional activation of several genes possibly mediated through CDK9/cyclin T (66, 67).

We have shown that multiple signaling pathways are affected when using combination drug therapy with trastuzumab and flavopiridol. There is some specificity to the targeted pathways controlling proliferation and apoptosis because we found that the abundance of certain cellular oncogenes (*e.g.,* cdc25A) and signal transduction proteins (*e.g.,* p38 and JNK) remains unchanged in control *versus* drug-treated cells. The ultimate goal of this combination approach is to reduce the abundance and activity of cyclin D1. This has been achieved at multiple levels as we have shown that there is a selective decrease in MAPK (ERK) signaling. Furthermore, we have shown that there is decreased activation of Akt, suggesting that additional mechanisms of repression of cyclin D1 activation may involve reduced stimulation of FRAP/mTOR kinase activity. Because the Akt pathway is implicated in cell cycle progression as well as apoptosis (*i.e.,* through alterations in Bad-Bax function), alterations in Akt function also induce cell death in addition to reducing proliferation. Because cyclin D1 plays an important role to promote both cell cycle progression and cellular survival and multiple pathways regulate cyclin D expression, drug combinations that exploit more than one pathway probably have the best success in producing cellular cell cycle arrest and death.

Acknowledgments

We acknowledge and are grateful for the constructive criticism and helpful suggestions of Drs. I. David Goldman (Albert Einstein Comprehensive Cancer Center) and David Bregman (Department of Pathology, Albert Einstein College of Medicine) in their review of the manuscript.

References

1. Lee, R. J., Albanese, C., Fu, M., D'Amico, M., Lin, B., Watanabe, G., Haines, G. K. I., Siegel, P. M., Hung, M. C., Yarden, Y., Horowitz, J. M., Muller, W. J., and Pestell, R. G. Cyclin D1 is required for transformation by activated Neu and is induced through an E2F-dependent signaling pathway. Mol. Cell. Biol., *20:* 672–683, 2000.

2. Slamon, D. J., Clark, G. M., Wong, S. G., Levin, W. J., Ullrich, A., and McGuire, W. L. Human breast cancer: correlation of relapse and survival with amplification of the HER-2/*neu* oncogene. Science (Wash. DC), *235:* 177–182, 1987.

3. Kurokawa, H. L. A., Simpson, J. F., Pisacane, P. I., Sliwkowski, M. X., Forbes, J. T., and Arteaga, C. L. Inhibition of HER2/neu (erbB-2) and mitogen-activated protein kinases enhances tamoxifen action against HER2-overexpressing, tamoxifen-resistant breast cancer cells. Cancer Res., *60:* 5887–5894, 2000.

4. Ciocca, D. R., and Eledge, R. Molecular markers for predicting response to tamoxifen in breast cancer patients. Endocrine, *13:* 1–10, 2000.

5. Yu, D., Liu, B., Tan, M., Li, J., Wang, S. S., Hung, M. Role of erbB2 in breast cancer chemosensitivity. Bioessays, *22:* 673–680, 2000.

6. Yu, D., Liu, B., Tan, M., Li, J., Wang, S. S., and Hung, M. C. Overexpression of c-erbB-2/neu in breast cancer cells confers increased resistance to Taxol via MDR-1-independent mechanisms. Oncogene, *19:* 1359–1365, 1996.

7. Baselga, J. Current and planned clinical trials with trastuzumab. Semin. Oncol., *27:* 27–32, 2000.

8. Janes, P. W., Daly, R. J., deFazio, A., and Sutherland, R. L. Activation of the Ras signalling pathway in human breast cancer cells overexpressing *erb*B-2. Oncogene, *9:* 3601–3608, 1994.

9. Muthuswamy, S. K., Siegel, P. M., Dankort, D. L., Webster, M. A., and Muller, W. J. Mammary tumors expressing the *neu* proto-oncogene possess elevated c-Src tyrosine kinase activity. Mol. Cell. Biol., *14:* 735–743, 1994.

10. Qian, Y-W., Wang, Y-C., Hollingsworth, R. E., Jones, D., Ling, N., and Lee, E. Y. A retinoblastoma-binding protein related to a negative regulator of Ras in yeast. Nature (Lond.), *364:* 648–652, 1993.

11. Pestell, R. G., Albanese, C., Reutens, A. T., Segall, J. E., Lee, R. J., and Arnold, A. The cyclins and cyclin-dependent kinase inhibitors in hormonal regulation of proliferation and differentiation. Endocr. Rev., *20:* 501–534, 1999.

12. Albanese, C., Johnson, J., Watanabe, G., Eklund, N., Vu, D., Arnold, A., and Pestell, R. G. Transforming p21^{ras} mutants and c-Ets-2 activate the cyclin D1 promoter through distinguishable regions. J. Biol. Chem., *270:* 23589–23597, 1995.

13. Westwick, J. K., Lambert, Q. T., Clark, G. J., Symons, M., Van Aelst, L., Pestell, R. G., and Der, C. J. Rac regulation of transformation, gene expression and actin organisation by multiple PAK-independent pathways. Mol. Cell. Biol., *17:* 1324–1335, 1997.

14. Lee, R. J., Albanese, C., Stenger, R. J., Watanabe, G., Inghirami, G., Haines, G. K. I., Webster, M., Muller, W. J., Brugge, J. S., Davis, R. J., and Pestell, R. G. pp60$^{v\text{-}src}$ induction of cyclin D1 requires collaborative interactions between the extracellular signal-regulated kinase, p38, and Jun kinase pathways: a role for cAMP response element-binding protein and activating transcription factor-2 in pp60$^{v\text{-}src}$ signaling in breast cancer cells. J. Biol. Chem., *274:* 7341–7350, 1999.

15. Bromberg, J. F., Wrzeszczynska, M. H., Devgan, G., Zhao, Y., Pestell, R. G., Albanese, C., and Darnell, J. E. *Stat3* as an oncogene. Cell, *98:* 295–303, 1999.

16. Matsumura, I., Kitamura, T., Wakao, H., Tanaka, H., Hashimoto, K., Albanese, C., Downward, J., Pestell, R. G., and Kanakura, Y. Transcriptional regulation of cyclin D1 promoter by STAT5: its involvement in cytokine-dependent growth of hematopoietic cells. EMBO J., *18:* 1367–1377, 1999.

17. Shtutman, M., Zhurinsky, J., Simcha, I., Albanese, C., D'Amico. M., Pestell, R., and Ben-Ze'ev, A. The *cyclin D1* gene is a target of the β-catenin/LEF-1 pathway. Proc. Natl. Acad. Sci. USA, *96:* 5522–5527, 1999.

18. D'Amico, M., Hulit, J., Amanatullah, D., Zafonte, B. T., Albanese, C., Maofu Fu, M., Ikui, A., Donehower, L. A., Shtutman, M., Ben-Ze'ev, A., Dedhar, S., Takemaru, K-I., Moon, R. T., and Pestell, R. G. The integrin-linked kinase regulates the *cyclin D1* gene through glycogen synthase kinase 3β and CREB-dependent pathways. J. Biol. Chem., *275:* 32649–32657, 2000.

19. Watanabe, G., Howe, A., Lee, R. J., Albanese, C., Shu, I-W., Karnezis, A. N., Zon, L., Kyriakis, J., Rundell, K., and Pestell, R. G. Induction of cyclin D1 by simian virus 40 small tumor antigen. Proc. Natl. Acad. Sci. USA, *93:* 12861–12866, 1996.

20. Diehl, J. A., and Sherr, C. J. A dominant negative cyclin D1 mutant prevents nuclear import of cyclin-dependent kinase 4 (CDK4) and its phosphorylation of CDK-activating kinase. Mol. Cell. Biol., *17:* 7362–7374, 1997.

21. Sherr, C. J. Cancer cell cycles. Science (Wash. DC), *274:* 1672–1677, 1996.

22. Weinberg, R. A. The retinoblastoma protein and cell cycle control. Cell, *81:* 323–330, 1995.

23. Yu, Q., Geng, Y., and Sicinski, P. Specific protection against breast cancers by cyclin D1 ablation. Nature., *411:* 1017–1021, 2001.

24. Kaur, G., Stetler-Stevenson, M., Sebers, S., Worland, P., Sedlacek, H., Myers, C., Czech, J., Naik, R., and Sausville, E. A. Growth inhibition with reversible cell cycle arrest of carcinoma cells by flavone L86-8275. J. Natl. Cancer Inst., *84:* 1736–1740, 1992.

25. Losiewicz, M. D., Carlson, B. A., Kaur, G., Sausville, E. A., and Worland, P. J. Potent inhibition of CDC2 kinase activity by the flavinoid L86-8275. Biochem. Biophys. Res. Commun., *210:* 589–595, 1994.

26. Worland, P. J., Kaur, G., Stetler-Stevenson, M., Sebers, S., Sartor, O., and Sausville, E. A. Alteration of the phosphorylation state of p34cdc2 kinase by the flavone L86-8275 in breast carcinoma cells. Correlation with decreased H1 kinase activity. Biochem. Pharmacol., *46:* 1831–1840, 1993.

27. Carlson, B. A., Dubay, M. M., Sausville, E. A., Brizuela, L., and Worland, P. J. Flavopiridol induces G_1 arrest with inhibition of cyclin-dependent kinase (cdk) 2 and cdk4 in human breast carcinoma cells. Cancer Res., *56:* 2973–2978, 1996.

28. Brusselbach, S., Nettelbeck, D. M., Sedlacek, H. H., and Muller, R. Cell cycle-independent induction of apoptosis by the anti-tumor drug flavopiridol in endothelial cells. Int. J. Cancer, *77:* 146–152, 1998.

29. Bible, K. C., and Kaufmann, S. H. Flavopiridol: a cytotoxic flavone that induces cell death in noncycling A549 human lung carcinoma cells. Cancer Res., *56:* 4856–4861, 1996.

30. Parker, B. W., Kaur, G., Nieves-Neira, W., Taimi, M., Kohlhagen, G., Shimizu, T., Losiewicz, M. D., Pommier, Y., Sausville, E. A., and Senderowicz, A. M. Early induction of apoptosis in hematopoietic cell lines after exposure to flavopiridol. Blood, *91:* 458–465, 1998.

31. Patel, V., Senderowicz, A. M., and Decio, P. Flavopiridol, a novel cyclin-dependent kinase inhibitor, suppresses the growth of head and neck squamous cell carcinomas by inducing apoptosis. J. Clin. Investig., *102:* 1674–1681, 1998.

32. Senderowicz, A. M., Headlee, D., Stinson, S. F., Lush, R. M., Kalil, N., Villalba, L., Hill, K., Steinberg, S. M., Figg, W. D., Tompkins, A., Arbuck, S. G., and Sausville, E. A. Phase I trial of continuous infusion flavopiridol, a novel cyclin-dependent kinase inhibitor, in patients with refractory neoplasms. J. Clin. Oncol., *16:* 2986–2999, 1998.

33. Stadler, W. M., Vogelzang, N. J., Amato, R., Sosman, J., Taber, D., Liebowitz, D., and Vokes, E. E. Flavopiridol, a novel cyclin-dependent kinase inhibitor, in metastatic renal cell cancer: a University of Chicago Phase II Consortium Study. J. Clin. Oncol., *18:* 371–375, 2000.

34. Mani, S., Wang, C., Francis, R., and Pestell, R. G. Cyclin-dependent kinase inhibitors: novel anti-cancer drugs. Exp. Opin. Investig. Drugs, *9:* 1849–1870, 2000.

35. Zwijsen, R. M. L., Klompmaker, R., Wientjens, E. B. H. G. M., Kristel, P. M. P., van der Burg, B., and Michalides, R. J. A. M. Cyclin D1 triggers autonomous growth of breast cancer cells by governing cell cycle exit. Mol. Cell. Biol., *16:* 2554–2560, 1996.

36. Musgrove, E. A., Lee, C. S., Buckley, M. F., and Sutherland, R. L. Cyclin D1 induction in breast cancer cells shortens G1 and is sufficient for cells arrested in G1 to complete the cell cycle. Proc. Natl. Acad. Sci. USA, *91:* 8022–8026, 1994.

37. Carlson, B., Lahusen, T., Singh, S., Loaiza-Perez, A., Worland, P. J., Pestell, R., and Sausville E. Downregulation of cyclin D1 by transcriptional repression in MCF-7 human breast carcinoma cells induced by flavopiridol. Cancer Res., *59:* 4634–4641, 1999.

38. Chou, T-C., and Talalay, P. Quantitative analysis of dose-effect relationships: the combined effects of multiple drugs or enzyme inhibitors. Adv. Enzyme Regul., *22:* 27–55, 1984.

39. Bible, K. C., and Kaufmann, S. H. Cytotoxic synergy between flavopiridol (NSC 649890, L86-8275) and various antineoplastic agents: the importance of sequence of administration. Cancer Res., *57:* 3375–3380, 1997.

40. Pegram, M., and Lewis, G. Inhibitory effects of combinations of HER-2/neu antibody and chemotherapeutic agents used for treatment of human breast cancers. Oncogene, *18:* 2241–2251, 1999.

41. Alessi, D. R., Cuenda, A., Cohen, P., Dudley, D. T., and Saltiel, A. R. PD 098059 is a specific inhibitor of the activation of mitogen-activated protein kinase kinase *in vitro* and *in vivo*. J. Biol. Chem., *270:* 27489–27494, 1995.

42. Le, X. F., McWatters, A., Bae, D. S., Mills, G. B., Kumar, R., and Bast, R. C., Jr. Differential signaling by an anti-p185(HER2) antibody and heregulin. Cancer Res., *60:* 3522–3531, 2000.

43. Wang, C., Fu, M., D'Amico, M., Albanese, C., Brownlee, M., Lisanti, M. P., Chatterjee, K., Lazar, M. A., and Pestell, R. G. Inhibition of cellular proliferation through $I\kappa B$ kinase independent and $PPAR\gamma$ receptor dependent repression of cyclin D1. Mol. Cell. Biol., *219:* 3057–3070, 2001.

44. Van den Heuvel, S., and Harlow E. Distinct role for cyclin dependent kinases in cell cycle control. Science (Wash. DC), *262:* 2050–2054, 1993.

45. Zafonte, B., Amanatullah, D., Sage, D., and Pestell, R. G. Ras regulation of cyclin dependent immunoprecipitation kinase assays. *In:* W. E. Balch, C. J. Der, and A. Hall (eds.), Methods in enzymol regulators and effectors of small GTPases, Vol. 322, pp. 116–124. San Diego: Academic Press, 2001.

46. Lybarger, L., Dempsey, D., Franek, K. J., and Chervenak, R. Rapid generation and flow cytometric analysis of stable GFP-expressing cells. Cytometry, *25:* 211–220, 1996.

47. Choi, M. Mechanism of transforming growth factor-β1 signaling: role of the mitogen-activated protein kinase. Kidney Int., *58:* 53–58, 2000.

48. Douziech, N., Calvo, E., Laine, J., and Morisset, J. Activation of MAP kinases in growth responsive pancreatic cancer cells. Cell Signalling, *11:* 591–602, 1999.

49. Bouzahzah, B., Fu, M., Iaavarone, A., Factor, V. M., Thorgeirsson, S. S., and Pestell, R. G. Transforming growth factor β1 recruits histone deacetylase 1 to a p130 repressor complex in transgenic mice *in vivo*. Cancer Res., *60:* 4531–4537, 2000.

50. Amundadottir, L. T., and Leder, P. Signal transduction pathways activated and required for mammary carcinogenesis in response to specific oncogenes. Oncogene, *16:* 737–746, 1998.

51. Pinkas-Kramarski, R., Soussan, L., Waterman, H., Levkowitz, G., Alroy, I., Klapper, L., Lavi, S., Seger, R., Ratzkin, B. J., Sela, M., and Yarden, Y. Diversification of Neu differentiation factor and epidermal growth factor signaling by combinatorial receptor interactions. EMBO J., *15:* 2452–2467, 1996.

52. Wallasch, C., Weiss, F. U., Niederfellner, G., Jallal, B., Issing, W., and Ullrich, A. Heregulin-dependent regulation of HER2/neu oncogenic signaling by heterodimerization with HER3. EMBO J., *14:* 4267–4275, 1995.

53. Galaktionov K., and Beach, D. Specific activation of cdc25 tyrosine phosphatases by B-type cyclins: evidence for multiple roles of mitotic cyclins. Cell, *67:* 1181–1194, 1991.

54. Hoffman, I., Dreatta, G., and Karsenti, E. Activation of the phosphatase activity of human cdc25A by a cdk2-cyclin E dependent phosphorylation at the G1/S transition. EMBO J., *13:* 4302–4310, 1994.

55. Blomberg, I., and Hoffman., I. Ectopic expression of cdc25A accelerates the G1/S transition and leads to premature activation of cyclin E-and cyclin A-dependent kinases. Mol. Cell. Biol., *19:* 6183–6194, 1999.

56. Slikowski, M. X., Lewis, G. D, Hotaling, T. E., Fendly, B. M., and Fox, J. A. Nonclinical studies addressing the mechanism of action of trastuzumab (Herceptin). Semin. Oncol., *26* (Suppl. 12)*:* 60–70, 1999.

57. Nelson, J. M., and Fry, D. W. Akt, MAPK (Erk 1/2), and p38 act in concert to promote apoptosis in response to ErbB receptor family inhibition. J. Biol. Chem., *276:* 14842–14847, 2001.

58. Busse, D., Doughty, R., Ramsey, T. T., Russell, W. E., Price, J. O., Flanagan, W. M., Shawver, L. K., and Arteaga, C. L. Reversible G_1 arrest induced by inhibition of the epidermal growth factor receptor tyrosine kinase requires up-regulation of p27(KIP1) independent of MAPK activity. J. Biol. Chem., *275:* 6987–6995, 2000.

59. Nakamura, N., Vazquez, F., Vazquez, F., Signoretti, S., Loda, M., and Sellers, W. R. Forkhead transcription factors are critical effectors of cell death and cell cycle arrest downstream of PTEN. Mol. Cell. Biol., *20:* 8969–8982, 2000.

60. Graff, J. R., McNulty, A. M., Wang, Z., Houck, K., Allen, S., Paul, J. D., Hbaiu, A., Goode, R. G., Sandusky, G. E., Vessella, R. L., and Neubauer, B. L. Increased Akt activity contributes to prostate cancer progression by dramatically accelerating prostate tumor growth and diminishing p27Kip1 expression. J. Biol. Chem., *11:* 24500–24505, 2000.

61. Gingras, A. C., Kennedy, S. G., O'Leary. M. A., Sonenberg, N., and Hay, N. 4E-BP1, a repressor of mRNA translation, is phosphorylated and inactivated by the Akt(PKB) signaling pathway. Genes Dev., *15:* 502–513, 1998.

62. Muise-Helmericks, R. C., Grimes, H. L., Bellacosa, A., Malstrom, S. E., Tsichlis, P. N., and Rosen, N. J. Cyclin D expression is controlled post-transcriptionally via a phosphatidylinositol 3-kinase/Akt-dependent pathway. J. Biol. Chem., *6:* 29864–29872, 1998.

63. Kaiser, A., Nishi, K., Gorin, F. A., Walsh, D. A., Bradbury, E. M., and Schnier, J. B. The cyclin-dependent kinase (CDK) inhibitor flavopiridol inhibits glycogen phosphorylase. Arch. Biochem. Biophys., *386:* 179–187, 2001.

64. Boerner, S. A., Tourne, M. E., Kaufmann, S. H., and Bible, K. C. Effect of P-glycoprotein on flavopiridol sensitivity. Br. J. Cancer, *84:* 1391–1396, 2001.

65. Bible, K. C., Bible, R. H., Kottke. T. J., Svingen, P. A., Xu, K., Pang, Y. P., Hajdu, E., and Kaufmann, S. H. Flavopiridol binds to duplex DNA. Cancer Res., *60:* 2419–2428, 2000.

66. Chao, S. H., and Price, D. H. Flavopiridol inactivates P-TEFb and blocks most RNA polymerase II transcription *in vivo*. J. Biol. Chem., *276:* 31793–31799, 2001.

67. Chao, S. H., Fujinaga, K., Marion, J. E., Taube, R., Sausville, E. A., Senderowicz, A. M., Peterlin, B. M., and Price, D. H. Flavopiridol inhibits P-TEFb and blocks HIV-1 replication. J. Biol. Chem., *275:* 28345–28348, 2000.